Performance Evaluation of ERA5 Reanalysis against Radiosonde Observations in Representing Atmospheric Vertical Variability on a Seasonal Scale in the Maritime Continent of Indonesia

Muhizzadin Abdul Adzan[1], Pertiwi Risky Setyowatri[1], Yosafat Donni Haryanto[1]*

[1]Meteorology Study Program, College of Meteorology Climatology and Geophysics, Tangerang, Tangerang City, Banten, Indonesia

Email: muhizzadin12@gmail.com, pertiwirisky118@gmail.com, *yosafat.haryanto@stmkg.ac.id

Received: 30nd January 2026; Revised: 04th June 2026; Accepted: 22th July 2026

Abstract – *ERA5 reanalysis is widely applied in meteorological studies, but its performance requires evaluation in regions with complex seasonal dynamics such as the Indonesian Maritime Continent (BMI). This study assesses the ability of ERA5 to represent seasonal atmospheric vertical variability using radiosonde observations. The analysis covers December 2021 to November 2024 at three stations, namely Soekarno-Hatta, Juanda, and I Gusti Ngurah Rai, for temperature, relative humidity, zonal wind, and meridional wind at eight standard pressure levels from 925 to 100 hPa. Evaluation methods include Hovmöller analysis, Mean Absolute Error (MAE), Mean Error (ME), correlation coefficient, scatter plots, and box plots for December–January–February (DJF), March–April–May (MAM), June–July–August (JJA), and September–October–November (SON) seasons. Results indicate that ERA5 represents temperature very well, with MAE values of 0.3 to 1.1°C and correlations exceeding 0.9, although errors increase at 100 hPa. Wind components also show high correlations above 0.9 but exhibit underestimated amplitudes, particularly for zonal winds during DJF. In contrast, relative humidity shows good agreement in the lower layers but significant limitations in the upper layers, with MAE values up to 58 percent, correlations below 0.6, and overestimation above 300 hPa. These findings confirm ERA5's reliability for temperature and wind analyses, while humidity remains a key source of uncertainty in tropical maritime regions.*

Keywords: *ERA5 reanalysis; evaluation; Indonesian maritime continent; radiosonde; seasonal.*

1. Introduction

Modern atmospheric reanalyses, particularly ERA5 developed by the European Centre for Medium-Range Weather Forecasts (ECMWF), have become one of the main sources of data in weather and climate studies due to their high spatial and temporal resolution and long historical coverage [1]. ERA5 provides three-dimensional atmospheric variables with hourly temporal resolution and finer horizontal resolution than previous-generation reanalysis products, enabling a more realistic representation of cross-scale atmospheric dynamics. The advantages of this resolution can enhance the ability of reanalysis to capture mesoscale structures, which are atmospheric phenomena with spatial scales of approximately 2–2,000 km such as convective systems and squall lines, as well as near-surface atmospheric processes that previously posed a major challenge for coarse-resolution reanalyses. In various climatological and meteorological applications, ERA5 has been widely used as a substitute for in-situ observations, particularly in regions with limited or uneven observation networks, such as the open ocean, the Arctic, Africa, and parts of Southeast Asia [2, 3].

However, reanalysis data is essentially a synthesis of numerical models and observations, and therefore is not free from systematic and random uncertainties. These uncertainties stem from limitations in data assimilation schemes, the representation of physical processes, model resolution, and the scarcity and imbalance of the distribution of assimilated observations [4]. Radiosondes, as upper-air observations with very high vertical resolution of around five to eight metres, are still considered the most reliable reference for evaluating geopotential temperature, humidity and wind profiles at various pressure levels [5]. Radiosonde-based evaluation is crucial because even small biases in certain layers can accumulate and have a significant impact on downstream applications such as numerical forecasting. Previous studies have shown that reanalysis uncertainty increases in regions with sparse observation coverage and complex interactions between land and atmosphere, highlighting the importance of local radiosonde-based evaluation [6].

A number of previous studies have examined the performance of ERA5 against radiosondes in various regions and climatological contexts. An evaluation of five reanalysis products based on radiosonde observations over the Central Taklimakan Desert shows that ERA5 outperforms ERA-Interim, JRA-55, MERRA-2, and NCEP2 in describing geopotential height, specific humidity, and wind components [6]. The study also revealed that the largest errors tended to occur in the lower layer around 850 hPa, which is associated with the complexity of land-atmosphere interactions and the limitations of the model in representing surface processes. These findings confirm that although ERA5 is relatively superior, vertical bias is still significant and is greatly influenced by regional characteristics.

Another study evaluated the performance of several reanalysis products, including ERA5, MERRA-2, JRA-55, and CRA40, compared with radiosonde observations in China for weighted mean temperature (Tm) estimates [7]. The results show that ERA5 has the smallest error with an RMSE of approximately 1.69 K and the highest correlation with radiosondes, and that the increased spatial resolution of ERA5 consistently improves accuracy. However, this study also highlights the existence of error variations influenced by latitude and elevation, indicating that ERA5's performance is not spatially or temporally homogeneous. In other words, the global superiority of ERA5 does not automatically guarantee optimal accuracy at every pressure level and in every seasonal regime.

In the context of the Indonesian Maritime Continent, the challenge of evaluating ERA5 becomes more complex because this region is characterised by intense tropical convection driven by high sea surface temperatures and abundant moisture flux, strong land-sea interactions that generate diurnal convective cycles over islands and coastal zones, and the Asia-Australia monsoon system that dominates annual rainfall[8]. Monsoonal seasonal variations, namely the boreal rainy season (DJF), the first transition season (MAM), the boreal dry season (JJA), and the second transition season (SON), produce sharp changes in the thermodynamic and atmospheric dynamics, especially in the lower to middle troposphere [9]. These characteristics have the potential to increase reanalysis bias at certain pressure levels, particularly in coastal areas and international airports located in land-sea transition zones, such as Soekarno Hatta, Juanda, and I Gusti Ngurah Rai. However, to date, studies that systematically evaluate ERA5 biases and correlations with radiosondes at various pressure levels in the Indonesian Maritime Continent region, with a separation of the DJF, MAM, JJA, and SON seasons, are still very limited.

Although various studies have proven the relative superiority of ERA5 over other reanalysis products, there is a clear research gap regarding the vertical and seasonal validation of ERA5 in the BMI region. Most previous evaluations were conducted in mid-latitude or continental desert regions, which have atmospheric dynamics that are very different from those of the Indonesian Maritime Continent. Therefore, this study aims to evaluate the bias and correlation of ERA5 with radiosondes at various pressure levels at the Soekarno-Hatta, Juanda, and I Gusti Ngurah Rai Meteorological Stations, taking into account the seasonal variations of the DJF, MAM, JJA, and SON monsoons. This approach is expected to provide a more accurate understanding of ERA5 performance in the BMI region and provide a strong scientific basis for the use of ERA5 in regional climate studies and numerical model development in Indonesia.

2. Material and Method

This study was conducted at three main stations representing the coastal and maritime regions of the Indonesian Maritime Continent, namely the Soekarno-Hatta Meteorological Station in Banten, the Juanda Meteorological Station in East Java, and the I Gusti Ngurah Rai Meteorological Station in Bali, as shown in Figure 1. These three stations were selected because they have relatively continuous radiosonde data availability and are located in areas with monsoonal rainfall patterns. The analysis period covers the period from December 2021 to November 2024 (3 years). This time frame was chosen to capture monsoonal seasonal variability and significant intra-annual fluctuations in tropical regions.

The data used in this study consists of ERA5 hourly data on single levels (https://cds.climate.copernicus.eu/) and radiosonde upper air observation data obtained through Wyoming at the three station locations (https://weather.uwyo.edu/upperair/). The atmospheric parameters analysed include temperature, relative humidity, zonal wind direction (U), and meridional wind (V). The evaluation was conducted at eight standard pressure levels, namely 925, 850, 700, 500, 400, 300, 200, and 100 hPa, representing the lower, middle, and upper troposphere. All data were analysed on a monsoonal seasonal scale, namely December-January-February (DJF), March-April-May (MAM), June-July-August (JJA), and September-October-November (SON) to examine the variation in bias and the performance of ERA5 against radiosondes under different atmospheric dynamics conditions.

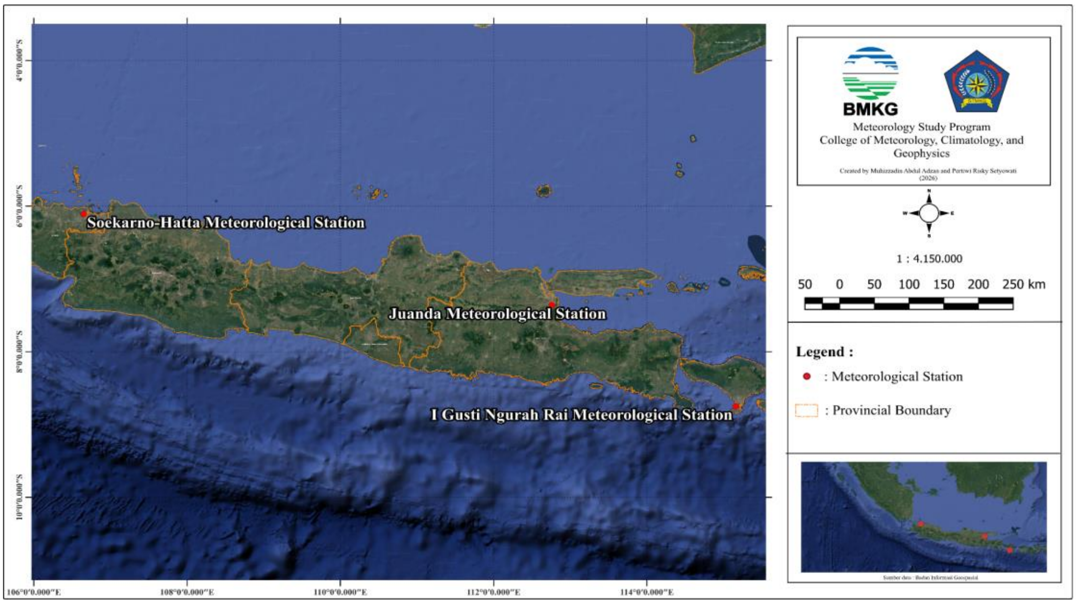

Figure 1. Research map.

The evaluation of ERA5 performance against radiosondes was carried out using evaluation metrics for each layer, scatter plots, box plots, and visualisation of radiosonde data with Hovmöller plots. The evaluation metrics used were Mean Absolute Error (MAE), Mean Error (ME), and correlation coefficient (R) on the scatter plot graph. MAE was used because it shows the direct average value of the error of each point, so this measure is unambiguous and directly represents the average error and is more stable against outliers [10]. ME is used because it measures the direction of the average bias of the model, particularly indicating the tendency to overestimate, underestimate, or not bias the observation data [11]. The correlation coefficient (R) is used to assess the level of conformity of the variation pattern between ERA5 and radiosonde at each pressure layer and season [12]. The equations used are MAE in Equation (1), ME in Equation (2), boxplots in Equations (3) to (4) to find the quartiles and lower/upper limits, scatter plots in Equations (5) to (6), and Equation (7) describes the average time from the hourly data at each station.

$$MAE = \frac{1}{N}\sum_{i=1}^{N}|M_i - O_i| \quad (1)$$

$$ME = \frac{1}{N}\sum_{i=1}^{N}(M_i - O_i) \quad (2)$$

$$Q_1 = P_{25},\ Q_2 = P_{50},\ Q_3 = P_{75}, IQR = Q_3 - Q_1 \quad (3)$$

$$Lower\ Whisker = Q_1 - 1.5\,IQR \text{ and } Upper\ Whisker = Q_3 + 1.5IQR \quad (4)$$

$$y = ax + c \quad (5)$$

$$R = \frac{\sum_{i=1}^{N}(M_i-\overline{M})(O_i-\overline{O})}{\sqrt{\sum_{i=1}^{N}(M_i-\overline{M})^2\sum_{i=1}^{N}(O_i-\overline{O})^2}} \quad (6)$$

$$X_{t,k} = \frac{1}{N_{t,k}}\sum_{i=1}^{N_{t,k}} X_i \quad (7)$$

Description:

M_i : ERA5 model parameter value at observation-i
O_i : Radiosonde observation parameter value at observation-i
$\overline{M}$: ERA5 model average value
$\overline{O}$: Radiosonde observation average value
N : Number of valid data pairs (without missing data)
Q_i : The quartile-i
IQR : Interquartile Range (50%)
y : ERA5 model value
a : Slope indicating the sensitivity of the model to observations
c : Regression intercept
X_i : All hourly average data for each station
$N_{t,k}$: Number of valid data pairs (without missing data).

3. Results and Discussion

3.1. Hovmöller diagram of radiosonde data

A visualisation of the vertical conditions of radiosonde parameters consisting of air temperature, relative humidity, zonal wind, and meridional wind in the form of a Hovmöller diagram at three stations in Indonesia is shown in Figure 2. The figure represents the relationship between time vs pressure levels for specific parameters [13, 14]. Based on the figure, in the temperature column, each station shows insignificant temperature variations in each layer (horizontal). As shown in Figure 2a, there is a vertical temperature gradient, with relatively warm temperatures in the lower layer (925–700 hPa) ranging from 13 to 29°C, and progressively cooler temperatures in the middle to upper layers, reaching as low as −89°C to below 6°C. This vertical gradient arises because solar radiation primarily heats the Earth's surface, warming the air above it through sensible heat flux and long-wave radiation, while temperatures decrease with altitude following the rate of environmental temperature decline due to the adiabatic cooling rate of the rising air parcel [15, 16]. In tropical regions such as the Maritime Continent of Indonesia, this vertical contrast is particularly pronounced because intense surface heating driven by high sea surface temperatures sustains strong convective activity, whereas the horizontal temperature gradient remains relatively small due to nearly uniform radiative forcing at low latitudes [17].

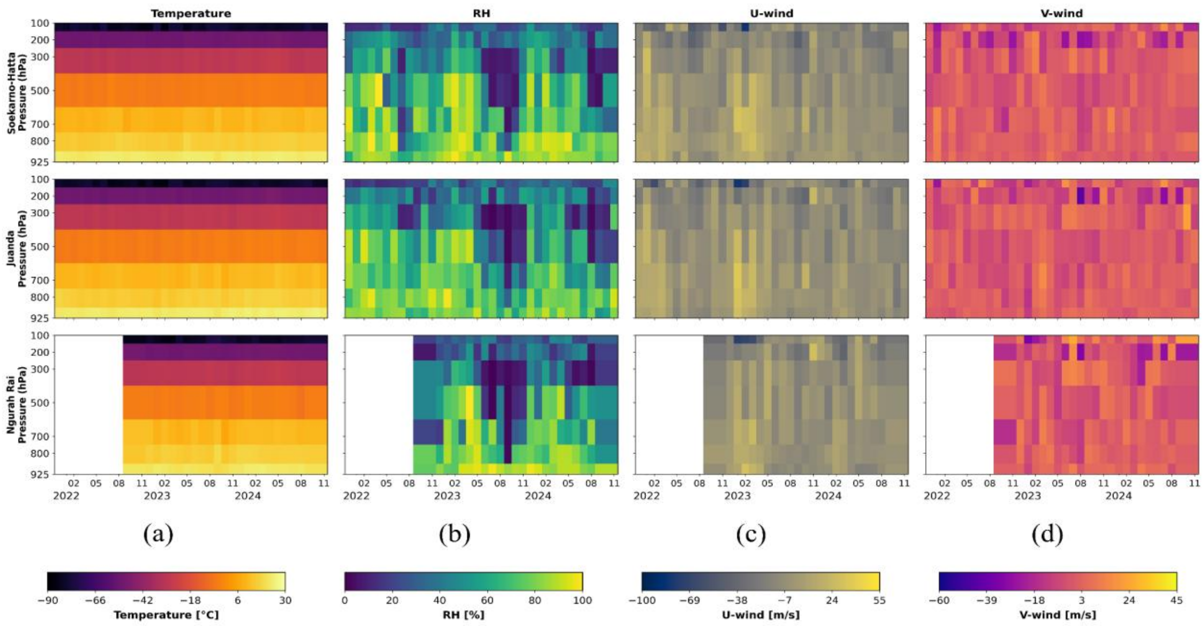

Figure 2. Hovmöller diagrams of radiosonde data for (a) temperature, (b) relative humidity, (c) zonal wind, and (d) meridional wind at three stations: Soekarno-Hatta (first row), Juanda (second row), and Ngurah Rai (third row).

Furthermore, based on the relative humidity (RH) parameters in Figure 2.b, contrasting temporal patterns are observed at the three stations, with low RH values (approximately 6–55%) during the MAM, JJA, and SON seasons and a tendency for humidity to increase during the DJF season, particularly up to the 300 hPa level. This pattern is physically consistent with the dominance of the Asia-Australia monsoon system over the Indonesian Maritime Continent, where the boreal winter (DJF) is controlled by the Asian monsoon, which transports large amounts of water vapor from the South China Sea and warm tropical sea surfaces toward the Indonesian region, thereby intensifying convective activity and increasing atmospheric water vapor content up to the middle troposphere [18, 19]. Conversely, during the JJA, the Australian monsoon brings dry continental air masses from the Australian mainland, which suppresses convection and reduces humidity throughout the atmospheric column [20].
Furthermore, based on zonal wind parameters (U), variations in wind speed over time indicate that the Asian monsoon wind pattern causes positive zonal winds (towards the east), while the Australian monsoon period causes negative zonal winds (towards the west) [21]. In addition, based on meridional winds (V), the relatively diverse wind patterns may indicate the influence of other regional or global phenomena, which can affect monsoon patterns [22]. However, in general, meridional wind patterns show positive values in the Australian monsoon and negative values in the Asian monsoon, as well as relatively more diverse patterns during the transition period [23].

3.2. MAE evaluation of pressure levels

The evaluation of the four parameters was carried out using the Mean Absolute Error (MAE) evaluation matrix for atmospheric layer heights and differentiated based on seasonal periods, as visualised in Figure 3. Based on the temperature graph, the MAE values ranged from 0.3 to 1.1 °C, with a tendency for the error to decrease from the 925 to 200 hPa layer, then increase sharply at the 100 hPa layer. This pattern is in line with previous studies showing that temperature errors in the lower layers are relatively greater, decrease in the middle layers, and increase again in the upper layers [24]. The MAE variation at the three stations shows insignificant seasonal differences in height. Furthermore, based on the relative humidity graph, the MAE values were in the range of 5–58%, with relatively small errors in the lower to middle layers (925–500 hPa) and showing an increasingly steep gradient towards the 100 hPa layer, especially above an altitude of 300 hPa. These findings are consistent with previous studies showing an increase in relative humidity error in the upper layers of the atmosphere [24]. The pattern of MAE variation between seasons relative to altitude is relatively uniform, with the JJA season showing the smallest error values.

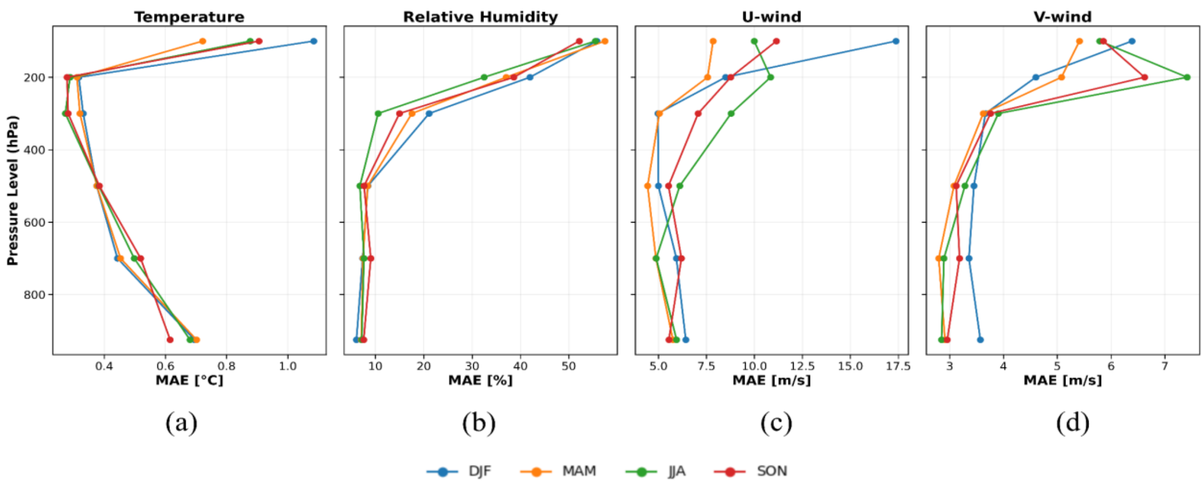

Figure 3. MAE graph of the ERA5 model against radiosonde for the parameters of (a) temperature, (b) relative humidity, (c) zonal wind, and (d) meridional wind for the DJF, MAM, JJA, and SON seasons.

Furthermore, based on the zonal wind (U) graph, the MAE value range is between 4–17.5 m/s with a relatively varied downward pattern up to the 100 hPa layer. The largest MAE value occurs in the DJF season, while a relatively smaller value is found in the MAM season. Furthermore, based on the meridional wind MAE (V) graph, the MAE value interval was in the range of 2–8 m/s with a relatively uniform decrease from the 925 to 300 hPa layer, then decreasing more steeply in the layers above (>300 hPa). In general, the meridional wind MAE values were smaller than those of the zonal wind. The MAM season showed the lowest average MAE values for meridional winds compared to other seasons.

3.3. ME evaluation of pressure levels

In addition to using MAE, evaluation was also conducted using Mean Error (ME) to identify the bias tendency of ERA5 data towards radiosonde data at the three stations, as shown in Figure 4. Based on the temperature graph, the average difference interval between ERA5 and radiosonde fluctuates in the range of −6 to 0.2 °C, with a tendency to underestimate in the lower to middle layers, and overestimate in layers above 200 hPa, except in the 100 hPa layer in the DJF season. In the relative humidity (RH) graph, the ME value ranges from approximately −1 to 58%, with values relatively close to zero in the 925–500 hPa layer, then increasing sharply and showing a tendency to overestimate in the layers above. This is also reported in relation to ERA5 humidity data compared to radiosonde data [24].

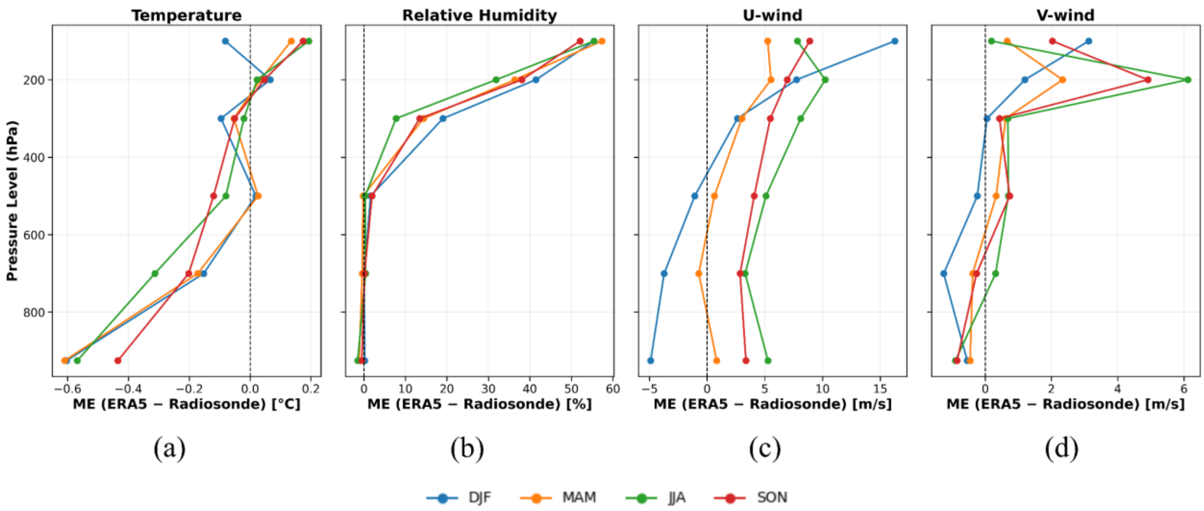

Figure 4. ME graph of the ERA5 model against radiosonde for the parameters of (a) temperature, (b) relative humidity, (c) zonal wind, and (d) meridional wind for the DJF, MAM, JJA, and SON seasons.

Furthermore, based on the zonal wind (U) graph, the ME interval ranges from −5 to 16 m/s, with most seasons showing an overestimation tendency, except for the lower layer of the DJF season and the 700 hPa layer in the MAM season. The DJF season shows the greatest variation in zonal wind. Meanwhile, based on the meridional wind (V) graph, ME variation ranges from −1.2 to 6.2 m/s, with an underestimate tendency at the surface layer and shifting to an overestimate starting at the 500 hPa layer. The MAM season shows the smallest meridional wind ME variation. These findings are in line with previous studies which explain that errors in zonal winds generally have a larger range than meridional winds, which are associated with excessive easterly biases due to the model's limitations in representing the drag mechanism of mesoscale convection and the neglect of surface ocean currents, which have been shown to contribute significantly to reducing zonal flow speeds [25].

3.4. Scatterplot evaluation of seasons

In simultaneously identifying the consistency of variation patterns between ERA5 and radiosonde data, as well as the level of model value conformity to observation data, ERA5 performance evaluation at the three stations was conducted using scatter plots as shown in Figure 5. Based on the temperature scatter plots for each season, the correlation coefficient (R) is close to 1, indicating that ERA5 can capture the patterns of variation in radiosonde temperature data relatively well, meaning that the increase and decrease trends in ERA5 closely follow those observed in the radiosonde measurements. In addition, a gradient value of 0.99 indicates that the model's temperature estimates are relatively close to the radiosonde data. This finding is in line with previous studies reporting temperature gradients greater than 0.9, indicating that temperature variations can be well represented by the ERA5 model [12]. The distribution of red dots shows a clustering pattern at certain temperature values, which is related to the use of standard pressure layers, resulting in contrasting vertical variations. Furthermore, based on the relative humidity (RH) scatter plot, it can be seen that the distribution of blue dots tends to be on the left side of the dotted line, indicating a tendency to overestimate the model data. R values in the range of 0.34–0.59 indicate that the model's ability to represent RH variation patterns is relatively lower than that for temperature, especially in the DJF season. In addition, regression line gradient values in the range of 0.27–0.63 indicate a lower rate of increase in model amplitude values relative to radiosonde data, with the lowest gradient occurring in the DJF season.

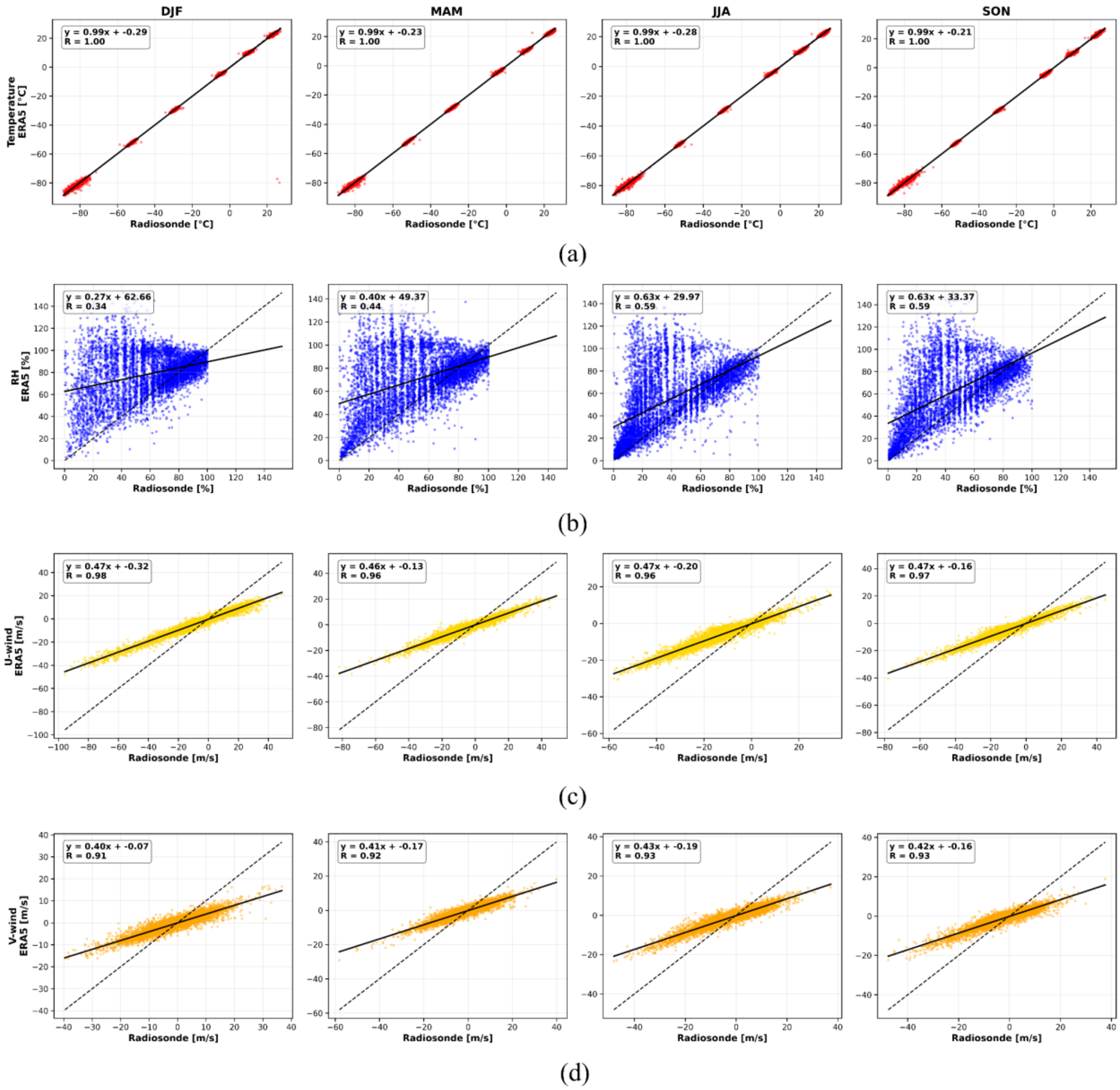

Figure 5. Seasonal scatter plot (DJF, MAM, JJA, and SON) between the ERA5 model and radiosonde data for (a) temperature, (b) relative humidity, (c) zonal wind, and (d) meridional wind parameters.

Based on the zonal wind (U) scatter plot, the distribution pattern of the yellow dots shows that the model tends to overestimate the radiosonde at negative speeds and relatively underestimate it at positive speeds. The R value for each season is in the range of 0.96–0.98, indicating that the variation pattern (increase and decrease) of the model closely resembles the variation pattern of the radiosonde data. However, the relatively uniform gradient values for each season, around 0.46–0.47, indicate that the amplitude of the zonal wind produced by the model tends to be underestimated compared to the radiosonde, where an increase of 1 m/s in the radiosonde is only followed by an increase of around 0.47 m/s in the model. Furthermore, based on the meridional wind (V) scatter plot, the distribution pattern of the relationship between the model and the radiosonde shows characteristics similar to those of the zonal wind. The R value is in the range of 0.91–0.93, which indicates that the pattern of variation (increase and decrease) of the model is relatively consistent with the variation in radiosonde data. However, the meridional wind gradient value, which is in the range of 0.40–0.43, shows that the rate of increase in the model value is still lower than the radiosonde data.

3.5. Evaluation of error distribution with boxplots

In addition to using scatter plots to identify the distribution of data errors, analysis was also performed using boxplots to evaluate the characteristics of error distribution, including the first quartile (Q1), median (Q2), third quartile (Q3), interquartile range (IQR), and whiskers, as shown in Figure 6 [26]. Based on the temperature boxplot, it can be seen that the IQR distribution (50% of the middle data) is in a relatively narrow interval, namely around −1 to 1. The existence of outliers in almost all lower whisker and upper whisker values in each season indicates that most of the errors are concentrated in a small range, so that the whisker length is relatively short and extreme values can be identified more clearly [27]. Furthermore, based on the relative humidity (RH) boxplot, the IQR distribution shows that 50% of the median error data is in the range of approximately 0–40, with the largest interval occurring in the DJF season. The largest outlier variation was identified in the JJA season, with maximum and minimum values reaching approximately 140% and −80%, respectively.

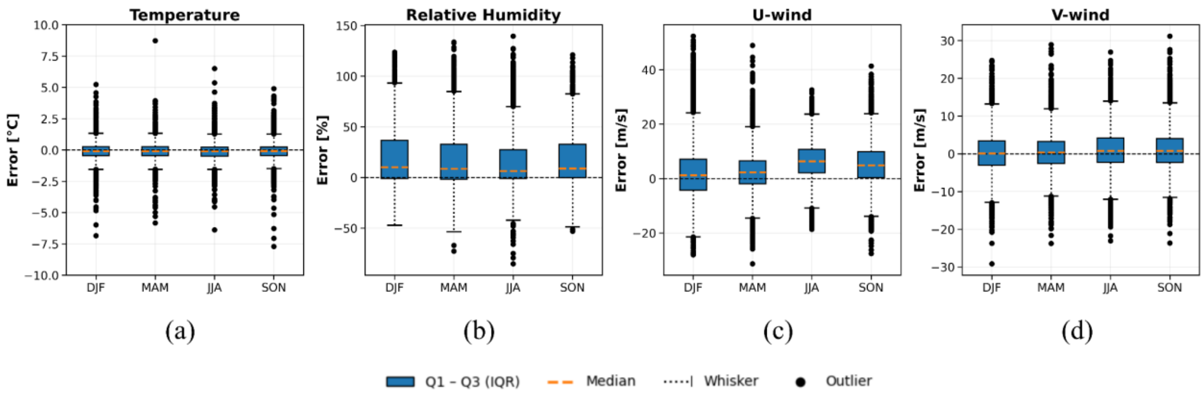

Figure 6. Boxplot of the distribution of ERA5 model errors against radiosonde data for (a) temperature, (b) relative humidity, (c) zonal wind, and (d) meridional wind parameters in the DJF, MAM, JJA, and SON seasons.

Furthermore, based on the zonal wind (U) boxplot, 50% of the median data shows inter-seasonal variation, with the largest interval occurring in the DJF season, which is around −5 to 6. In this season, the outlier values also reached the most extreme range (around −30 to 48), followed by the MAM season. In contrast, the JJA season shows the smallest IQR and outlier range, indicating that the model is relatively better at representing zonal winds than other seasons. Furthermore, based on the meridional wind (V) boxplot, the IQR distribution shows relatively uniform variation between seasons, namely around −3 to 4 m/s. The distribution of extreme values in each season is also relatively consistent, indicating that the variation in ERA5 errors relative to radiosondes in the meridional wind component is seasonally stable. This condition indicates the influence of regional and global atmospheric dynamics that play a role in modulating wind characteristics in the Indonesian region.

4. Conclusion

The analysis results show that ERA5 is generally capable of representing the vertical structure of the atmosphere in the Indonesian region, particularly for temperature and wind parameters. Temperature performance is best in the middle pressure levels (200–500 hPa) with MAE values as low as 0.3°C, while errors increase in the lower layers around 925 hPa (MAE up to 1.1°C) and rise sharply at 100 hPa. For wind components, the meridional wind shows the smallest errors with MAE in the range of 2–8 m/s and best performance during the MAM season, while zonal wind errors are largest during DJF with MAE reaching up to 17.5 m/s. Hovmöller visualisation confirms the dominance of vertical gradients over horizontal temperature variations typical of tropical regions, as well as the strong influence of the monsoon system on the distribution of humidity and wind components. The very high correlation in temperature and wind (R > 0.9) across all pressure levels confirms ERA5's ability to capture atmospheric variability patterns, although the amplitude of the variation tends to be underestimated, particularly in the wind component with regression gradients of approximately 0.46 for zonal wind and 0.41 for meridional wind. On the other hand, ERA5's performance in terms of relative humidity remains a major weakness across all evaluated stations. Although MAE values are relatively small in the lower to middle layers (925–500 hPa, approximately 5–15%), errors increase significantly above 300 hPa, reaching up to 58%, with low correlations below 0.6 and a consistent overestimation tendency as indicated by both ME and scatter plot analyses. The wide and asymmetric error distributions in the boxplot analysis, particularly during the DJF season, further confirm the existence of systematic biases that vary between pressure levels and seasons. These findings indicate that the representation of convective processes, water vapour transport, and cloud dynamics in ERA5 still has considerable limitations in the complex tropical maritime environment of the Indonesian Maritime Continent.

Acknowledgments

We would like to express our gratitude to the Meteorology, Climatology, and Geophysics Agency (BMKG) as the provider of radiosonde data, the University of Wyoming as the provider of supporting data sources, and the Copernicus Climate Change Service (C3S) for providing ERA5 data, which has contributed significantly to the smooth running and quality of this research. Appreciation is also extended to the State College of Meteorology Climatology and Geophysics (STMKG) for the facilitation, guidance, and scientific support provided during the implementation of this research.

References

[1] Hersbach H, Bell B, Berrisford P, Hirahara S, Horányi A, Muñoz-Sabater J, Nicolas J, Peubey C, Radu R dan Schepers D 2020 The ERA5 global reanalysis. Q. J. R. Meteorol. Soc. 146 1999–2049
[2] Gbode I E, Babalola T E, Diro G T dan Intsiful J D 2023 Assessment of ERA5 and ERA-interim in reproducing mean and extreme climates over West Africa Adv. Atmos. Sci. 40 570–86
[3] Gleixner S, Demissie T dan Diro G T 2020 Did ERA5 improve temperature and precipitation reanalysis over East Africa? Atmosphere (Basel). 11 996
[4] Compo G P, Whitaker J S, Sardeshmukh P D, Matsui N, Allan R J, Yin X, Gleason B E, Vose R S, Rutledge G dan Bessemoulin P 2011 The twentieth century reanalysis project Q. J. R. Meteorol. Soc. 137 1–28
[5] Guo J, Zhang J, Yang K, Liao H, Zhang S, Huang K, Lv Y, Shao J, Yu T dan Tong B 2021 Investigation of near-global daytime boundary layer height using high-resolution radiosondes: First results and comparison with ERA-5, MERRA-2, JRA-55, and NCEP-2 reanalyses Atmos. Chem. Phys. Discuss. 2021 1–39
[6] Huang J, Yin J, Wang M, He Q, Guo J, Zhang J, Liang X dan Xie Y 2021 Evaluation of five reanalysis products with radiosonde observations over the Central Taklimakan Desert during summer Earth Sp. Sci. 8 e2021EA001707
[7] Sun Y, Yang F, Liu M, Li Z, Gong X dan Wang Y 2023 Evaluation of the weighted mean temperature over China using multiple reanalysis data and radiosonde Atmos. Res. 285 106664
[8] Nogueira M 2020 Inter-comparison of ERA-5, ERA-interim and GPCP rainfall over the last 40 years: Process-based analysis of systematic and random differences J. Hydrol. 583 124632
[9] Wu C-H, Lee S-Y, Chiang J C H dan Tsai P-C 2023 Role of precession on the transition seasons of the Asian monsoon npj Clim. Atmos. Sci. 6 95
[10] Hodson T O 2022 Root mean square error (RMSE) or mean absolute error (MAE): When to use them or not Geosci. Model Dev. Discuss. 2022 1–10
[11] Mugume I, Basalirwa C, Waiswa D, Reuder J, Mesquita M d S, Tao S dan Ngailo T J 2016 Comparison of parametric and nonparametric methods for analyzing the bias of a numerical model Model. Simul. Eng. 2016 7530759

[12] Hassan R M, Salah Z, Karacostas T dan Abdel-Wahab M M 2023 Assessment of reanalysis datasets against radiosonde observation over the Eastern Mediterranean region Acta Geophys. 71 2989–3005
[13] Hocke K dan Kämpfer N 2011 Hovmöller diagrams of climate anomalies in NCEP/NCAR reanalysis from 1948 to 2009 Clim. Dyn. 36 355–64
[14] Persson A 2017 The story of the Hovmöller diagram: An (almost) eyewitness account Bull. Am. Meteorol. Soc. 98 949–57
[15] Hartmann D L, Dygert B D, Blossey P N, Fu Q and Sokol A B 2022 The Vertical Profile of Radiative Cooling and Lapse Rate in a Warming Climate *J. Clim.* 35 6253–65
[16] Gettelman A and Forster P M de F 2002 A Climatology of the Tropical Tropopause Layer. *J. Meteorol. Soc. Japan. Ser. II* 80 911–24
[17] Bao J dan Stevens B 2021 The elements of the thermodynamic structure of the tropical atmosphere J. Meteorol. Soc. Japan. Ser. II 99 1483–99
[18] Tangang F, Chung J X, Juneng L, Supari, Salimun E, Ngai S T, Jamaluddin A F, Mohd M S F, Cruz F, Narisma G, Santisirisomboon J, Ngo-Duc T, Van Tan P, Singhruck P, Gunawan D, Aldrian E, Sopaheluwakan A, Grigory N, Remedio A R C, Sein D V., Hein-Griggs D, McGregor J L, Yang H, Sasaki H and Kumar P 2020 Projected future changes in rainfall in Southeast Asia based on CORDEX–SEA multi-model simulations *Clim. Dyn.* 55 1247–67
[19] Darmawan Y, Hsu H-H and Yu J-Y 2021 Characteristics of Large-Scale Circulation Affecting the Inter-Annual Precipitation Variability in Northern Sumatra Island during Boreal Summer *Atmosphere (Basel).* 12 136
[20] Zaini A Z A, Vonnisa M, Marzuki M dan Ramadhan R 2023 Seasonal Variation of Rainfall in Indonesia under Normal Conditions without ENSO and IOD Events from 1981-2021 J. Penelit. Pendidik. IPA 9 9899–909
[21] Wheeler M C dan McBride J L 2005 Australian-Indonesian monsoon Intraseasonal variability in the atmosphere-ocean climate system (Springer) hal 125–73
[22] Pujiastuti T T dan Nurjaman N 2019 Peranan Cross Equatorial Northerly Surge Terhadap Dinamika Atmosfer Di Wilayah Indonesia Bagian Barat J. Sains Teknol. Modif. Cuaca 20 1–11
[23] Huang F, Xu Z dan Guo W 2019 Evaluating vector winds in the Asian-Australian monsoon region simulated by 37 CMIP5 models Clim. Dyn. 53 491–507
[24] Kuchinskaia O, Bryukhanov I, Penzin M, Ni E, Doroshkevich A, Kostyukhin V, Samokhvalov I, Pustovalov K, Bordulev I dan Bryukhanova V 2022 ERA5 reanalysis for the data interpretation on polarization laser sensing of high-level clouds Remote Sens. 15 109
[25] Belmonte Rivas M dan Stoffelen A 2019 Characterizing ERA-Interim and ERA5 surface wind biases using ASCAT Ocean Sci. 15 831–52
[26] Nuzzo R L 2016 The box plots alternative for visualizing quantitative data PM&R 8 268–72
[27] Gang B, Lin H dan Tong T 2025 Unifying boxplots: a multiple testing perspective arXiv Prepr. arXiv2510.20259.